

# JE-990 Discrete Operational Amplifier\*

DEANE JENSEN

*Jensen Transformers, North Hollywood, CA 91601, USA*

## 0 INTRODUCTION

The performance of a number of popular audio integrated-circuit operational amplifiers, such as the NE5534, HA2625, and LM318, has been described by Jung [1]. The present paper presents a *discrete* operational-amplifier circuit which exhibits lower noise voltage, distortion, gain error, output impedance, and response time (delay) as well as higher slew rate, output voltage, output current, phase margin (stability), and gain – bandwidth product than most of these integrated-circuit operational amplifiers and also than most earlier discrete operational amplifiers in common use for audio applications. The development of this amplifier, called the JE-990 operational amplifier, involved a careful mixture of textbooks, laboratory-collected data, and computer calculations and graphics. Its application may be considered where some of these parameters are to be improved.

- 1) Input stage for any application where the source impedance is 2500  $\Omega$  or less,
- 2) Line output amplifier for driving a 75- $\Omega$  load up to an rms voltage level re 0.775 V of +25 dB, which is an rms voltage of 13.8 V and a peak-to-peak voltage of 39 V,
- 3) Summing amplifier,
- 4) Active filters requiring a high degree of stability,
- 5) Laboratory preamplifier for extending the sensitivity of noise or distortion measurements.

You can build the circuit yourself from the schematic and parts list given here if you have the necessary equipment and determination, or you can obtain a list of known sources of manufactured 990 amplifier modules.<sup>1</sup>

The circuit is “public domain” and can be used for any purpose without license or permission. Beyond this text there are no available application notes specifically for the

JE-990, except for a technical data sheet on a 170-kHz bandwidth microphone input transformer (Jensen Transformers) designed for optimum noise performance with the JE-990 operational amplifier. Full-size detailed graphs of those shown in this text are available from the author.

## 1 GENERAL DESCRIPTION

The JE-990 operational amplifier is a discrete universal gain block in the standard single-triangle configuration with one noninverting input, one inverting input for feedback, and one single-ended output. The principal objective of the development was to synthesize a stable high-performance operational amplifier which would take advantage of the low-noise and matching characteristics of the National Semiconductor LM394 supermatch pair transistor [2] – [4].

## 2 NOISE CONSIDERATIONS

### 2.1 The Input Device

The LM394 is actually a monolithic integrated circuit with 100 transistors; 25 pairs (50 transistors) per section are randomly interconnected in parallel to take advantage of statistical variations and random cancellation of offsets. The matching ratios improve proportionally to the square root of the number of transistors. Extrinsic emitter and base resistances are much lower than those of other available transistors, either monolithic or discrete, giving extremely low noise. To guarantee long-term stability of matching parameters, gain, and noise, internal clamp diodes have been added across the emitter – base junction of each transistor. These prevent degradation from reverse-biased emitter current, the most common cause of field failures in matched devices. The parasitic isolation junction formed by the diodes also ensures complete isolation between devices by clamping the substrate region to the most negative emitter [2, 3].

\* Manuscript received 1979 July 9; revised 1979 Sept. 27.

<sup>1</sup> Send written request for 990 sources to: Jensen Transformers, 10735 Burbank Blvd., North Hollywood, CA 91601.

## 2.2 Optimizing the Input-Transistor Collector Current

To determine an optimum collector current for the LM394 input pair, we measured the noise performance in our laboratory from several samples, using models, techniques, and computer programs similar to those given by Motchenbacher and Fitchen [5]. Two measurements of the noise in a 20-kHz bandwidth, one with a shorted input and the other with a known source impedance, were taken at eight collector currents ranging from 400  $\mu\text{A}$  to 4 mA. The 20-kHz bandwidth data for each collector current were first converted to a value of noise-voltage spectral density and of noise-current spectral density with a noise-model program. Then a polynomial regression program was used to average out atypical variations in the samples and measurements.

The resulting smoothed noise-voltage spectral density versus collector current is shown in Fig. 1, and the noise-current spectral density versus collector current is shown in Fig. 2. From these data, values for five collector currents were used in the noise-model program to calculate the noise index versus source ac resistance for each of the five collector currents. Fig. 3 shows a plot of this calculation for the case where the two sections of an LM394 are used as a differential pair. Fig. 4 shows the case where the two sections of an LM394 are paralleled, and two of these constitute the differential pair. Note that using two devices instead of one results in a noise reduction of 0.5 dB for a source ac resistance of 125  $\Omega$  and of 1.0 dB for a source ac

resistance of 31.5  $\Omega$ . The value of the ac resistance in these graphs is the sum of the ac resistance at the noninverting input and the parallel value of the series and shunt feedback resistors.

It is important to note that the ac resistance of many sources is greater than the dc resistance. Furthermore only resistive sources are modeled in this calculation. With some magnetic devices (for instance, magnetic tape reproducing heads) both the reactance and the ac resistance rise with increasing frequency. For such devices a more complex model should be used, taking into account both the reactance of the source and the change of both resistance and reactance with frequency.

The graphic form of the data of Figs. 3 and 4 is useful to determine the optimum collector current for a range of source resistances. Our measurements agree with the published values [2] at those data points that coincide. Note that the value of 1.6 mA is a good balance for a low noise index at low impedances without an unnecessary increase at high impedances. This "highest reasonable" collector current favors a high slew rate of 18 V/ $\mu\text{s}$ , but causes a fairly high input bias current of 2.2  $\mu\text{A}$ .

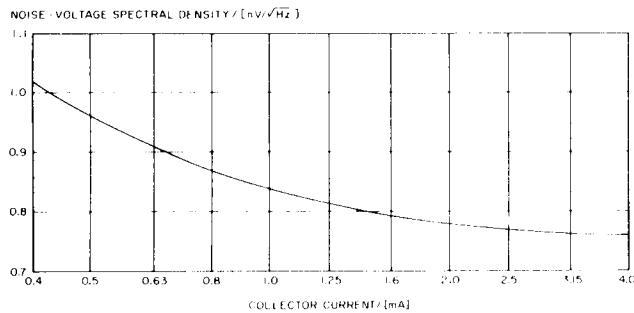


Fig. 1. Noise-voltage spectral density versus collector current for a single half-section of an LM394. Calculated from a measurement in a 20-kHz bandwidth.

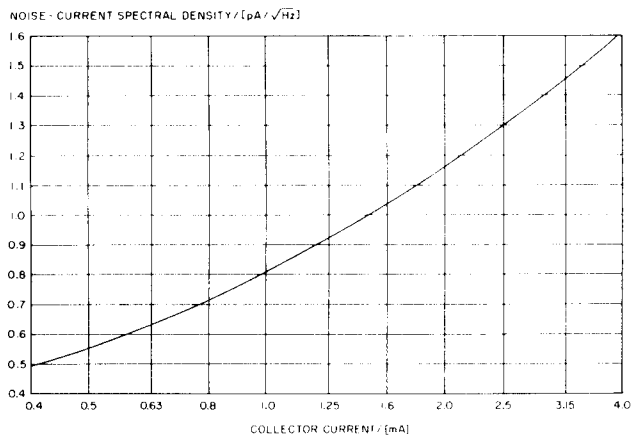


Fig. 2. Noise-current spectral density versus collector current for a single half-section of an LM394. Calculated from a measurement in a 20-kHz bandwidth.

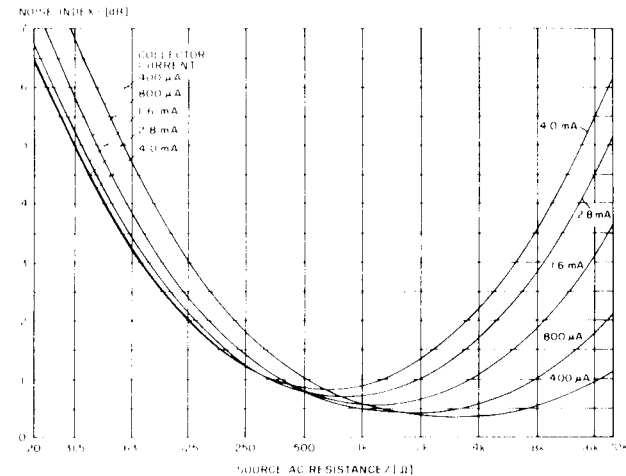


Fig. 3. Noise index versus source ac resistance for a differential pair of transistors, where each transistor is one half of an LM394. Calculated from a measurement in a 20-kHz bandwidth. Parameter: collector current.

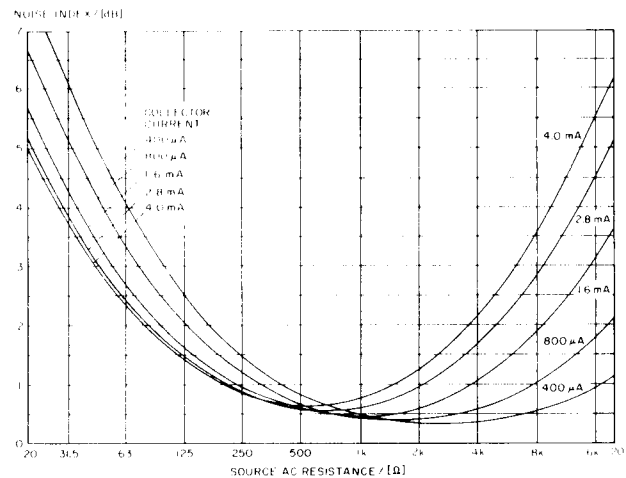


Fig. 4. Noise index versus source ac resistance for a differential pair of transistors, where each transistor is both halves of an LM394 in parallel. Calculated from a measurement in a 20-kHz bandwidth. Parameter: collector current.

With one LM394 at a collector current of 1.6 mA the noise voltage spectral density is 0.8 nV/√Hz per transistor, or 1.13 nV/√Hz for a differential pair; and a noise-current spectral density of 1.0 pA/√Hz yields a 0.6-dB noise index at the optimum source resistance of 1 kΩ. Above 8 kΩ the noise index exceeds 2 dB, and at 50 kΩ the noise index is 6 dB. So a high-impedance inductive source may exhibit rising high-frequency noise. The noise contribution of the second stage is less than 0.5 dB at unity gain.

The equivalent input noise voltage level of the complete JE-990 operational amplifier as a function of source ac resistance is shown in Fig. 5.

**2.3 Noise Measurement Filters and Corrections**

The noise measurement bandwidth was limited with an 8-pole (48-dB per octave) active low-pass filter [6]. To exclude hum from affecting the data, a single-pole high-pass filter at 800 Hz was used. This reduces the bandwidth of the measurement by 500 Hz [800 Hz/(π/2)], requiring a +0.11 dB correction to restore the data to 20-kHz bandwidth. The hum filter also removes the low-frequency 1/f noise of the amplifier. We verified, however, that the 1/f noise of the JE-990 operational amplifier contributes an insignificant part of the noise for the total 20-kHz bandwidth.

The voltmeter used was a Hewlett-Packard 400 FL, which is an average responding rectifier with a scale calibrated for the rms value of a sine wave. For the Gaussian noise waveform a correction level of +1.05 dB has been added to give the equivalent rms value of noise voltage.

**2.4 Preventing Noise Due to the Emitter Resistors**

The noise graphs shown for the LM394 do not include the noise due to the emitter resistors which are required to limit the gain-bandwidth product of the first stage in the case that someone connects the input to a zero-impedance source. If this is done without sufficient emitter resistance, the time delay of the other stages will cause insufficient phase margin of the first stage for unity-gain stability and ac

urate transient response. Emitter resistors of 30 Ω are required for high-frequency stability, but these increase the noise voltage level more than 3 dB above the case without emitter resistors. To prevent this noise increase, emitter inductors can be placed in parallel with the emitter resistors. The impedance of 20-μH inductors is 30 Ω at 240 kHz; so at higher frequencies the emitter circuit impedance is 30Ω. But at 10 kHz the 20-μH, 25-mΩ inductor lowers the emitter circuit impedance to 1.3 Ω. This reduces the noise voltage level in a 20-kHz bandwidth to within 0.4 dB of the case without emitter resistors.

The emitter impedance of the LM394 at a collector current of 1.6 mA is 16 Ω. This results in a first-stage single-pole response up to 83 kHz, where the 20-μH and 10.4-Ω impedance zero creates a two-pole response to 240 kHz, where the 20-μH and 30-Ω impedance pole creates a response zero, returning the response to that of a single pole.

**3 STABILITY ANALYSIS**

**3.1 Open-Loop Response Compensation**

The schematic of the JE-990 operational amplifier is shown in Fig. 6. Tobey et al. [7] and Roberge [8] discuss stability analysis in detail. The phase margin criterion for a "universal gain block" suggested the merits of a Miller-compensated two-stage amplifier. Initially the poles requiring compensation were located by observing the unity gain transient response while adjusting R9. The frequencies were input as the coefficients of a transfer function given in the Hewlett-Packard Transfer Function Analysis program. The output is a selection of topologies with values to synthesize the response function. With the zero of R9 and C1 coinciding with the unity-gain frequency  $f_1$ , the synthesis is completed in the emitter circuit of Q6 with C2, C3, and R8. The amplifier was constructed and analyzed in the laboratory to document the resulting unity-gain frequency  $f_1$ , phase margin, and transient response. Then an iterative series of calculations, component changes, and measurements was used to adjust the frequencies of the three zeros and the pole of the compensation circuit to obtain optimum phase margin and transient response. This method ensures that any response characteristics not isolated and identified in the modeling are nevertheless included in the optimization.

The result uses a capacitor and a series RC network across the emitter resistor of Q6 to create two zeros, one at 3.3 MHz and one at 25.4 MHz, with a pole at 5.8 MHz. The zero of R9 and C1 is at 8.1 MHz. The H-P AC Circuit Analysis (CNAP) program was used to model the response and to balance the impedance ratio of the feedback and emitter circuits of the second stage to give a 45° phase margin by adjusting  $f_1$  to approximately 1/8T, where T is the amplifier response time.

The resulting response magnitude (Fig. 7) and phase angle (Fig. 8) show a unity-gain frequency  $f_1$  of 10 MHz with about 38° phase margin, increasing to above 60° below 2 MHz, including the region of the first-stage emitter circuit 83-kHz response pole and 240-kHz response zero. The gain-bandwidth product is greater than 50 MHz in the 10-kHz to 100-kHz range and 25 MHz in the 1-MHz range,

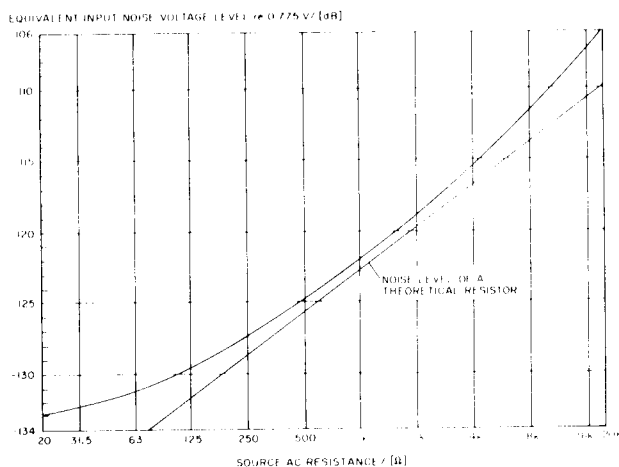


Fig. 5. Equivalent input noise voltage level of the complete JE-990 operational amplifier versus source ac resistance. Calculated from a measurement in a 20-kHz bandwidth. Noise level of a theoretical resistor is shown for reference.

with an increasing rate of attenuation to the actual frequency of unity gain, 10 MHz.

The transistors for Q5, type 2N4250A or PN4250A,

must have an input capacitance  $C_{ib}$  lower than the Jecdec specification in order to achieve the short response time which favors good phase margin, stability, and transient

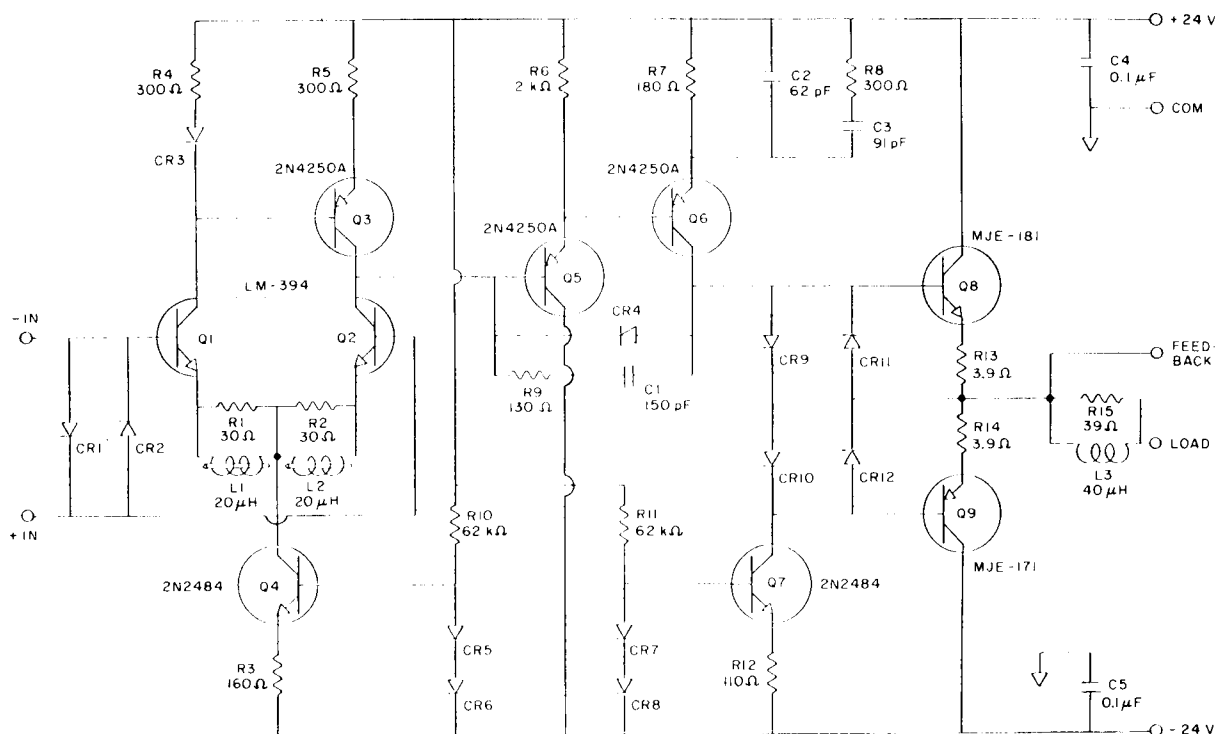


Fig. 6. Schematic drawing of the JE-990 operational amplifier.

JE-990 Operational Amplifier: Parts List

Quantity	Circuit #	Identification	Description	Manufacturer
1	Q1,2	LM-394H	Dual npn transistor	National Semiconductor
3	Q3,5,6	2N4250A,PN4250A	npn transistor	National Semiconductor or Fairchild
2	Q4,7	2N2484,PN2484	npn transistor	National Semiconductor or Fairchild
1	Q8	MJE-181 (1)	npn transistor	Motorola
1	Q9	MJE-171 (1)	npn transistor	Motorola
12	CR1-12	1N914B	Diode	Fairchild
2	R1,2	30 Ω	Resistor 5%, 1/4 W	Amperex film
1	R3	160 Ω	Resistor 5%, 1/4 W	Amperex film
3	R4,5,8	300 Ω	Resistor 5%, 1/4 W	Amperex film
1	R6	2 kΩ	Resistor 5%, 1/4 W	Amperex film
1	R7	180 Ω	Resistor 5%, 1/4 W	Amperex film
1	R9	130 Ω	Resistor 5%, 1/4 W	Amperex film
2	R10,11	62k Ω (2)	Resistor 5%, 1/4 W	Amperex film
1	R12	110 Ω	Resistor 5%, 1/4 W	Amperex film
2	R13,14	3.9 Ω	Resistor 5%, 1/4 W	Amperex film
1	R15	39 Ω (5)	Resistor 5%, 1 W	Allen Bradley
1	C1	150 pF 5%	Capacitor	
1	C2	62 pF 5%	Capacitor	
1	C3	91 pF 5%	Capacitor	
2	C4,5	0.1 μF	Capacitor CY20C104P	Centralab/USCC
2	L1,2	20 μH (4)	Shield bead 2673225111	Fair-Rite Prod.
1	L3	40 μH (5)	Inductor	
<i>Thermal Coupling Aids:</i>				
2	(1)	3/32 wire area	Clamp # C-201	Waldom
2	(1)	2-56 × 1/4	Screw # KF-461	Waldom
2	(1)	2-56 × 3/16 × 1/4	Nut # KF-554	Waldom
	(1)	4951 or 4952	Thermal adhesive	Thermalloy
1	(6)	256 D	Brass clip	Wakefield

- Notes: (1) CR9 must be thermally coupled to Q8 with clamp or adhesive.  
 CR10 must be thermally coupled to Q9 with clamp or adhesive.  
 (2) R10,11 = 62 kΩ for bipolar 24-V supply. R10,11 = 33 kΩ for bipolar 15-V supply.  
 (3) R4,5 may be trimmed for dc balance (also affects slew symmetry).  
 (4) L1,2 starter kit with sample assembly is available from Jensen.  
 (5) L3 (40 turns #30 wire wound around R15) is available assembled.  
 (6) Wakefield brass clip can be used to thermally couple two transistors for Q3 and CR3 (see text).

response. Fairchild and National Semiconductor have been tested and used; other types with the same part number cannot be safely substituted without analysis of the resulting response time and phase margin.

**3.2 Closed-Loop Response Compensation**

The JE-990 operational amplifier is unity-gain stable. The only overshoot remaining with a direct connection from the output to the inverting input is the servo overshoot caused by the amplifier response time of about 15 ns. If the circuit preceding the JE-990 is equivalent to a low-pass filter of 4 MHz or less, there is no overshoot at unity gain. Component variations may cause some ringing near 10 MHz, which can be minimized by adjusting the value of R9 by no more than 5%.

Feedback zero compensation as shown in Fig. 9 is recommended [8], [9]. A capacitor C<sub>f</sub> is connected across the series feedback resistor R<sub>f</sub> to create a phase lead (advance) in the feedback to avoid servo overshoot caused by the response time of the amplifier (about 15 ns). This delay causes the feedback to arrive late, during which time the output exceeds the equilibrium amplitude. Also the transient response at low closed-loop gain will exhibit overshoot if the inverted feedback transfer function (1/β) does not exhibit a pole at a frequency reasonably lower than the frequency of intercept with the open-loop response. The JE-990 will exhibit no overshoot with up to 45-dB closed-loop gain with feedback zero (phase lead) compensation in the feedback of τ<sub>f</sub> = R<sub>f</sub>C<sub>f</sub> = 1.3 μs. This yields a bandwidth of 120 kHz. The value of the capacitor is calcu-

lated as C<sub>f</sub> = 1.3 μs/R<sub>f</sub> [farads]. At 40-dB closed-loop gain, τ<sub>f</sub> = 0.9 μs for a bandwidth of 175 kHz.

For applications where 120-kHz bandwidth is sufficient, R<sub>f</sub> and C<sub>f</sub> can be fixed values, and R<sub>shunt</sub> can be adjusted to control closed-loop gain from 6 dB to 45 dB with nearly constant bandwidth and accurate transient response.

For applications where the maximum closed-loop gain required is less than 45 dB, the bandwidth can be increased by reducing the 1.3-μs time constant. The required compensation is determined initially by calculation from the frequency of intercept and the amount of feedback chosen for the frequency range above intercept [9]. Then the value is finalized by observing the small-signal transient response. The frequency of intercept is the intersection of the open-loop gain and the uncompensated inverted feedback function (1/β). The amount of feedback chosen for the frequency range above intercept could initially be set at 2 (6 dB) or 1.414 (3 dB). The pole frequency for the inverted feedback function is the intercept frequency divided by the feedback voltage ratio. Convert the frequency into a time constant by τ<sub>c</sub> = 1/(2πf). Then the compensation capacitor is determined by C<sub>f</sub> = τ<sub>c</sub>/R<sub>f</sub>. The value is fine-trimmed by observing the small-signal transient response.

If variable gain is realized by adjusting R<sub>f</sub> with R<sub>shunt</sub> fixed, the closed-loop response will always be close to the maximum allowable for stability and accurate transient response. Note that since the bandwidth and the gain do not track accurately at low closed-loop gain, the transient response must be observed at low gain to determine the maximum allowable gain – bandwidth that this method can realize.

Adjustment of R<sub>f</sub> with R<sub>shunt</sub> fixed yields maximum-bandwidth closed-loop response.

Adjustment of R<sub>shunt</sub> with R<sub>f</sub> fixed yields constant-bandwidth closed-loop response.

**4 SLEW RATE, DC BALANCE, AND LARGE-SIGNAL BANDWIDTH**

The slew rate of the JE-990 operational amplifier is 18 V/μs with a 150-Ω load and 16 V/μs with 75 Ω. The symmetry is a function of the match of R4 and R5 and the V<sub>be</sub> match of Q3 and CR3. These matches also affect the dc balance of the differential input stage. In the production of this circuit, these matches may require some monitoring. Fairchild 1N4148 diodes are very consistent, or a diode-connected transistor can be used for CR3. Thermal coupling should be considered for applications requiring dc stability. The match of R4 and R5 can be trimmed to adjust input offset current. Acceptable tolerances must be determined according to the application and component variations. If separate dc and ac (slew) balance adjustments are required, an ac-coupled shunt resistor across R4 or R5 will adjust the slew symmetry without affecting the dc balance.

The slew rate S is determined by the total available current I from the differential input stage, and the Miller compensation capacitor C1: S = I/C1. The current of the input stage has been set by the noise analysis at 1.6 mA per transistor, or total I = 3.2 mA, and the capacitor C1 = 150 pF, a value that cannot be reduced without affecting the

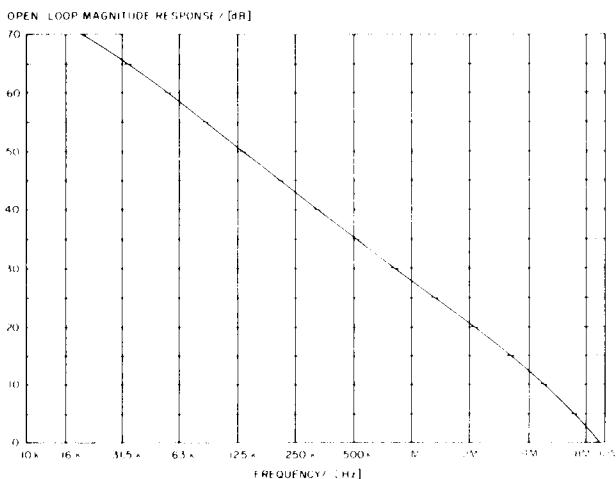


Fig. 7. Open-loop magnitude response of the JE-990 operational amplifier. Curve fit to the measured data.

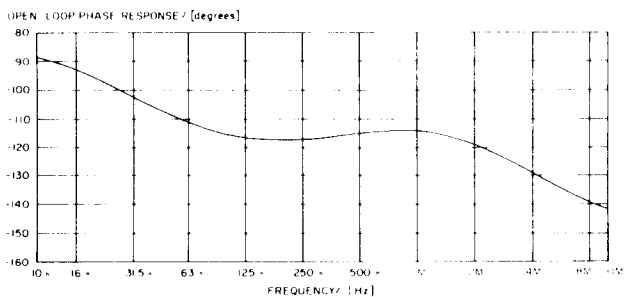


Fig. 8. Open-loop phase response of the JE-990 operational amplifier. Curve fit to the measured data.

symmetry of voltage overload (clipping). Thus  $S = 3.2 \text{ mA}/150 \text{ pF} = 21 \mu\text{V/s}$ . The impedance ratio of the feedback and emitter circuits of Q6 affects  $f_t$  which, for  $45^\circ$  phase margin, cannot exceed  $f_t = 1/8T$ , where  $T$  is the amplifier response time. So reduction of C1 will require an increase in the impedance of the emitter circuit components which would affect the symmetry of voltage overload. If this is done, R9 must also be increased to restore the zero to 8.1 MHz. Actually the iterative procedure to optimize the phase margin should be repeated. At higher slew rates the current set by R12 becomes a dominant limit to slew rate.

The "current-mirror" collector load for the first stage was chosen over the constant-current load for its factor-of-2 advantage in ac gain and available charging current for C1. The modified Darlington second stage was chosen over the straight Darlington for speed.

The large-signal bandwidth defined as  $B = S/2\pi E_{\text{peak}}$  is 145 kHz with a bipolar ( $\pm$ ) 24-V supply and 230 kHz with a bipolar ( $\pm$ ) 15 V supply.

## 5 OUTPUT STAGE

The Motorola 77-03 package output transistors were chosen for thermal and secondary breakdown performance over the TO-5 package types. At the relatively high quiescent collector current of 15 mA required for low distortion with a 75- $\Omega$  load, the higher speed TO-5 types failed the shorted-output tests even with heat sinks and yielded academically small improvements in distortion and response time. The biasing diodes CR9 and CR10 must be thermally coupled to Q8 and Q9, respectively, for low distortion with low-impedance loads. Even at quiescent current the temperature of the output transistors reduces the voltage drop of the diodes as part of the critical balance of multiple parameters determined by R12, R13, and R14. The current set by R12 in diodes CR9 and CR10 is 5.4 mA; it affects the slew rate and distortion with low load impedances. The resulting voltage drop across R13 and R14 determines the 15-mA quiescent current through Q8 and Q9, and this current sets lower limits on the open-loop performance of the output transistors: it controls their current gain, which in turn controls the open-loop output impedance, especially at high frequencies; it controls the frequency of unity gain  $f_t$ ; and it controls the time delay introduced by the transistors. At lower currents the output stage could introduce a pole below  $f_t$ , and this would reduce the phase margin.

### 5.1 Current Limiting CR11 and CR12

The value of R13 and R14 also affects the current-limit magnitude. When the output current reaches a value which is just less than the current corresponding to two-diode voltage drops divided by R13 or R14, the base current is starved to the output node by a three-diode path including CR9, CR10, and either CR11 or CR12.

Without heat sinks the MJE-171 and 181 transistors will reliably drive a full-level signal into a shorted output indefinitely. Thermal dissipation may be a packaging consideration.

### 5.2 Load Isolation R15 and L3

To isolate capacitive loads (in order to prevent them from reducing the phase margin by delaying the feedback) without significant losses in the operating frequency range, the parallel network of R15 and L3 is connected in series with the load only. The feedback is still derived from the output node before the load-isolation network. The 40- $\mu\text{H}$  inductance with the 39- $\Omega$  resistor exhibits an impedance pole at 155 kHz. Therefore the series impedance is 39  $\Omega$  above 155 kHz. But below 155 kHz the impedance decreases to about 0.2  $\Omega$  at dc. At 20 kHz the impedance is 5  $\Omega$  at  $80^\circ$ , resulting in only 0.11 dB loss with a 75- $\Omega$  load.

### 5.3 Clamp Diode CR4

Although the modified Darlington is preferred for speed, it does not prevent saturation of Q6 through feedback clamping as does the straight Darlington. The clamp diode CR4 restores that feature of the straight Darlington to the higher speed modified Darlington by starving the drive current to the base of Q5 when the collector of Q6 reaches the voltage of the base of Q6. This means that the amplifier will exhibit fast recovery from voltage overload (clipping).

## 6 OTHER CONSIDERATIONS

### 6.1 Anti-Latch-Up Diodes CR1 and CR2

The diodes CR1 and CR2 prevent signals faster than the response time of the amplifier from causing zero bias of either of the input transistors. If the feedback is too slow to maintain forward bias for either input transistor, one of the diodes CR1 or CR2 will provide bias from the input signal when the differential voltage reaches one-diode voltage drop. Without these diodes the output could latch up to either supply as a result of a steep input waveform.

### 6.2 Separate Regulators for Q4 and Q7

The separate regulators R10, CR5, and CR6 for Q4, and R11, CR7, and CR8 for Q7, prevent capacitive coupling and interaction between Q7 and Q4; such coupling would affect the phase margin.

### 6.3 Internal Decoupling C4 and C5

The internal high-frequency decoupling from the power supply ensures that any series losses in the connector or connection to the supply lines will not increase the impedance of the decoupling capacitors which are usually external to the basic "triangle" amplifier.

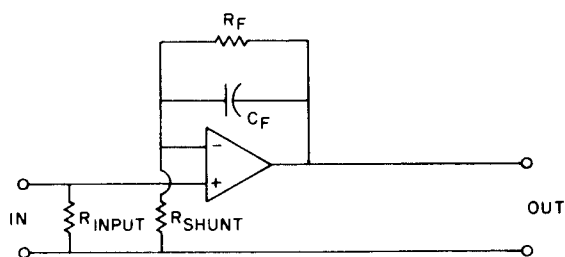


Fig. 9. Circuits of feedback components with zero compensation by means of  $C_f$ .

## 7 CONSTRUCTION

### 7.1 Layout Considerations

The node common to the collectors of Q2 and Q3, the base of Q5, CR4, and R9, is a very high impedance. Therefore this area should be made as small as possible. Shielding is suggested to avoid noise from external sources or response errors caused by capacitive coupling into this node. Parallel and symmetrical layout of the input section will yield improved common-mode rejection.

The collectors of Q8 and Q9 draw heavy currents. They should be connected to the supply terminals directly in order to prevent these currents from causing any IR drop in the resistances of the circuit-board foils which supply voltage to the other components in the circuit.

### 7.2 Emitter Inductor Construction

The emitter inductors are constructed by threading a piece of 250- $\mu\text{m}$  diameter (AWG 30) magnet wire through the six holes of a nickel-compound shield bead in an apparently noninductive pattern creating effectively one half turn, but with the characteristics of 57 mm (2.25 inches) of wire surrounded with a magnetic material of high permeability (2500). This construction is low in shunt capacitance and related self-resonance, which could alter the open-loop response and affect stability and transient response. Alternative constructions would require an analysis of the effects upon open-loop response, phase margin, and transient response.

## 8 PERFORMANCE OF THE JE-990 OPERATIONAL AMPLIFIER

Table 1 gives the values of the performance of the JE-990 operational amplifier which have been verified by multiple prototype measurements and calculations. The JE-990 is unity-gain stable and exhibits no overshoot up to 45 dB closed-loop gain, with 1.3- $\mu\text{s}$  phase lead compensation in the feedback circuit (bandwidth 120 kHz).

Also, Jung has kindly supplied us with his measurements of the total harmonic distortion under several test conditions, the equivalent input noise, and the frequency response at 60-dB gain. Jung's standard test setup [1] is shown in Fig. 10, and the test conditions and the purposes of the tests are summarized in Table 2. The results are shown in Fig. 11 for a 30-V ( $\pm 15$ -V) power supply and an rms output voltage of 7 V, and in Fig. 12 for a 48-V ( $\pm 24$ -V) power supply and an rms output voltage of 14 V. The detailed significance of these tests and comparative measurements for the integrated-circuit operational amplifiers  $\mu\text{A}741$ , NE5534, HA2625, LM318, RC4136, LF351, and LF356, are described in [1, sec. 2.4]. Note that the output linearity tests (G) are performed with a 2200- $\Omega$  load for all the integrated-circuit operational amplifiers, whereas the JE-990 is tested with a 150- $\Omega$  load. Also note that the integrated-circuit operational amplifiers are limited to a power-supply voltage of  $\pm 15$  V, whereas the JE-990 will operate up to a  $\pm 24$ -V supply. Therefore the JE-990 supplies about twice the maximum output voltage of the integrated-circuit operational amplifiers.

Table 1. Typical performance of the JE-990 operational amplifier

Quantity	Specification
Open-loop gain from dc to 30 Hz	125 dB
Gain error at 100-dB gain	0.4 dB
Noise-voltage spectral density:	
For each transistor	0.8 nV/ $\sqrt{\text{Hz}}$
For the differential pair	1.13 nV/ $\sqrt{\text{Hz}}$
Noise-current spectral density	1 pA/ $\sqrt{\text{Hz}}$
Noise index with a 1000- $\Omega$ source resistance	0.6 dB
Equivalent input noise voltage in a 20-kHz bandwidth with shorted input	160 nV
Corresponding voltage level re 0.775 V	-133.7 dB
Maximum input voltage at unity gain	13.8 V
Corresponding voltage level re 0.775 V	+25 dB
Input impedance, noninverting input	>10 M $\Omega$
Input bias current	+2.2 $\mu\text{A}$
Maximum output voltage with $R_L = 75 \Omega$	13.8 V
Corresponding voltage level re 0.775 V	+25 dB
Maximum peak output current	260 mA
Total harmonic distortion at 20 kHz, and an output voltage of 12.3 V (voltage level = +24 dB):	
$R_L = 75 \Omega$ , gain = 40 dB	0.06%
$R_L = 75 \Omega$ , gain = 20 dB	0.005%
$R_L = 600 \Omega$ , gain = 40 dB	0.015%
Slew rate:	
$R_L = 150 \Omega$	18 V/ $\mu\text{s}$
$R_L = 75 \Omega$	16 V/ $\mu\text{s}$
Large-signal bandwidth with $R_L = 150 \Omega$	145 kHz
Small-signal bandwidth at unity gain ( $f_u$ )	10 MHz
Gain-bandwidth product, in the frequency range 10 kHz to 100 kHz	>50 MHz
Phase margin:	
At 10 MHz	>38°
at <2 MHz	>60°
Response time at unity gain	<20 ns
Supply current with no load	25 mA
Supply voltage (bipolar)	$\pm 24$ V

The microphone preamplifier in Fig. 13 shows a typical application of the JE-990 with offset compensation and adjustable gain. The diode regulator and filter circuit supply a current into the inverting input which compensates for the offset caused by the unequal dc source resistances at the noninverting and the inverting inputs. The offset voltage at each input is first found by multiplying the input bias current (2.2  $\mu\text{A}$ ) by the dc source resistance at that input. For the noninverting input the dc-source resistance is the transformer secondary resistance paralleled by the load resistor. For the inverting input, the feedback resistor (10 k $\Omega$ ) is the only dc-source resistance path. Since the closed-loop dc gain of the amplifier is unity, the dc offset at the output is equal to the difference of the offset voltages at the two inputs. The compensation current required into the inverting input is the output-offset voltage divided by the feedback dc resistance (10 k $\Omega$ ).

This dc-offset compensation will significantly reduce the dc offset at the output for those applications without an output coupling capacitor.

The microphone preamplifier has a gain range of 12 dB to 45 dB with a bandwidth of 115 kHz.

## 9 REFERENCES

- [1] W. G. Jung, *Audio IC Op-Amp Applications*, no. 21558, Howard Sams, Indianapolis, 1978.
- [2] *Linear (Integrated Circuits) Data Book* (National

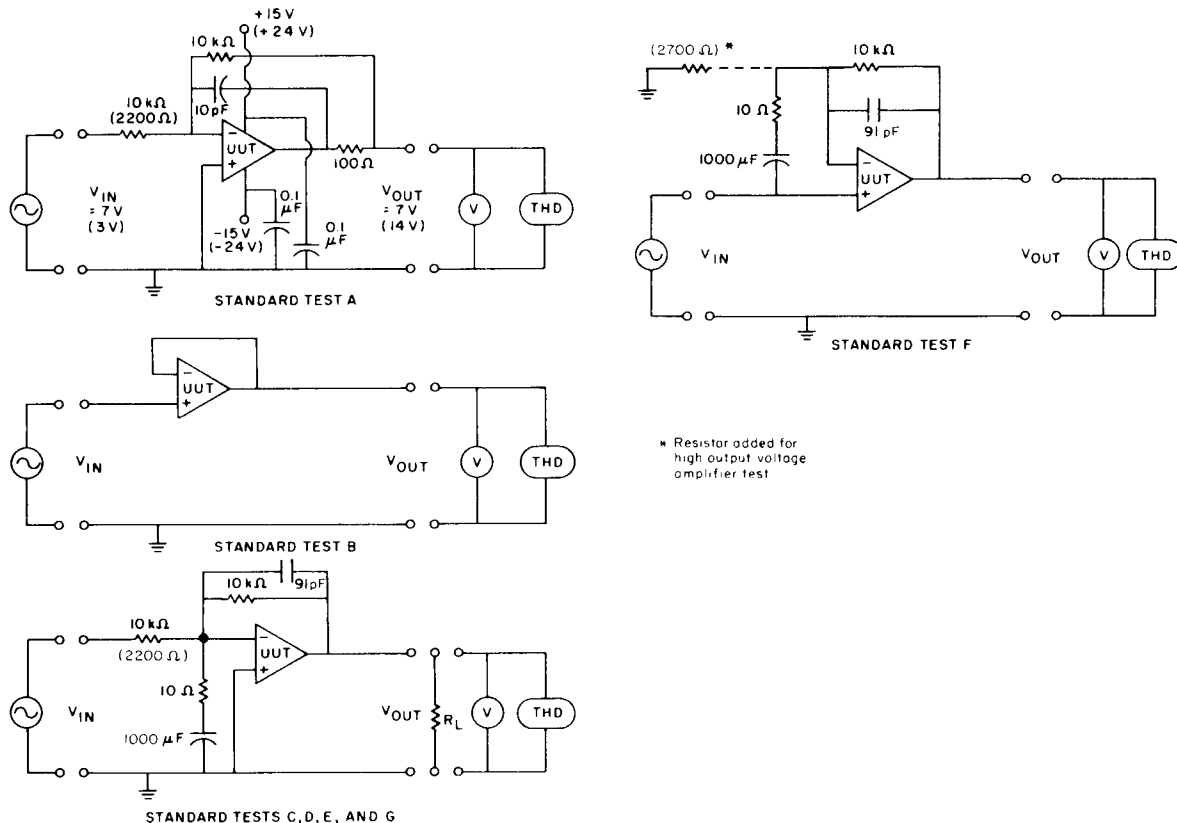


Fig. 10. Test setup for measurements according to Table 2. Values shown in parentheses for test A are typical of values used in all tests for the high-output-voltage (14-V) amplifier.

Table 2: Test series for operational-amplifier characterization [1].

Test	Test Object	General Conditions	Load	Frequency	Remarks
A	THD vs $f$ : Slew rate (general)	Unity gain,* inverting, with unity-gain compensation. Full rated output voltage. †	Open	100 Hz to 100 kHz (or to $f_p$ )	Checks slew rate independent of common-mode and output nonlinearities.
B	THD vs $f$ : Slew rate (common mode)	Unity gain,* noninverting, with unity-gain compensation. Full rated output voltage. †	Open	100 Hz to 100 kHz (or to $f_p$ )	Checks input common-mode slew rate if different than in test A.
C	Small-signal bandwidth	60-dB noise gain; inverting, unity signal gain,* compensation as appropriate. 1 V rms output.	Open	10 Hz to -3 dB point	Checks amplifier gain – bandwidth product to determine open-loop frequency response.
D	Noise	60-dB noise gain; compensation as appropriate. $R_s = 10 \Omega$ . No signal applied.	Open	Amplifier's bandwidth.	Measures equivalent input noise for low $R_s$ ; used to calculate spectral noise voltage density.
E	THD vs $f$ : Transfer linearity	60-dB noise gain; inverting, unity signal gain,* compensation as appropriate. Full rated output voltage. †	Open	10 Hz to 1/2 of -3 dB frequency	Checks basic transfer linearity of amplifier, independent of test A or B.
F	THD vs $f$ : Input nonlinearity	60-dB noise gain; noninverting, unity signal gain,* compensation as appropriate. Full rated output voltage. †	Open	10 Hz to 1/2 of -3 dB frequency	Checks input stage nonlinearity, independent of tests A, B and E.
G	THD vs $f$ : Output nonlinearity.	60-dB noise gain; inverting, unity signal gain,* compensation as appropriate. Full rated output voltage. † Rated $R_L$ .	IC's: 2 kΩ; JE-990: 150Ω	10 Hz to 1/2 of -3 dB frequency	Checks output stage nonlinearity, independent of tests A, B, E, and F.

\* For use with a  $\pm 24$  V power supply only: Since the test oscillator used would not deliver an input voltage of 14 V, which is necessary for the full output voltage test at unity gain, the gain was increased to 13.4 dB by changing the input resistor from 10 kΩ to 2200 Ω; thus an input voltage of 3 V would give an output voltage of 14 V for test A. For test B, a non-inverting gain of 13.4 dB was used.

† For integrated circuits and JE-990 with  $\pm 15$ -V supply voltage, rms output voltage = 7 V; for JE-990 with  $\pm 24$ -V supply rms output voltage = 14 V.



Semiconductor, Mountain View, CA, 1978).

[3] B. Cole, "IC Simulates Matched Transistor Pairs," *Electronics*, p. 141, (1976 Oct. 28).

[4] C. T. Nelson, "Super-Matched Transistor Pair . . .," Application Note 222, National Semiconductor Corp., Santa Clara, CA, 1979.

[5] C. D. Motchenbacher and F. C. Fitchen, *Low-Noise Electronic Design* (Wiley, New York, 1973).

[6] D. Jensen, "A 20 kHz Low Pass Filter for Audio Noise Measurements," *Record. Eng./Prod.*, vol. 8, no. 6, pp. 30-35 (1977 December).

[7] G. E. Tobey, J. R. Graeme, and L. P. Huelsman, *Operational Amplifiers, Design and Applications* (McGraw-Hill, New York, 1971).

[8] J. K. Roberge, *Operational Amplifiers, Theory and Practice* (Wiley, New York, 1975), chap. 8, "Operational Amplifier Design Techniques," and chap. 4, 5, and 13 on stability and compensation.

[9] D. Jensen, "Stabilizing Operational Amplifiers," *Record. Eng./Prod.*, vol 9, no. 3, pp. 42+ (1978 June).

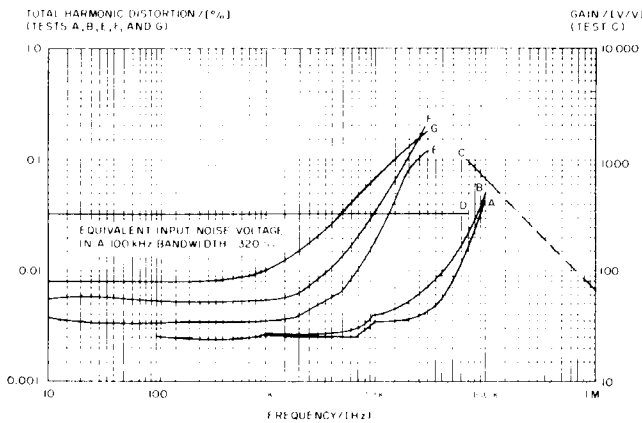


Fig. 11. Results of the measurements according to Table 2 for the JE-990 operational amplifier operating from a  $\pm 15\text{-V}$  supply, delivering an rms output voltage of 7 V into an open circuit, except for test G where a 150- $\Omega$  load is used.

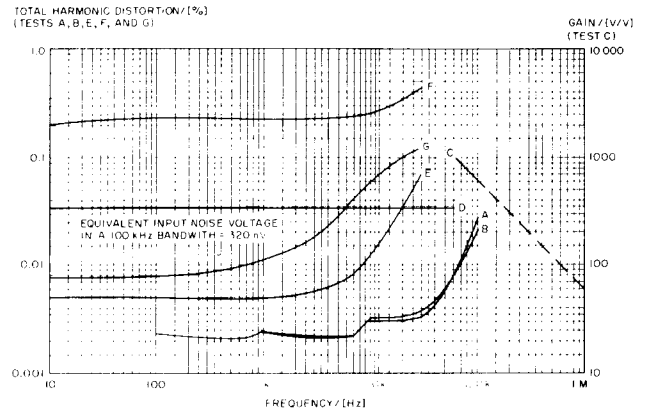


Fig. 12. Results of the measurements according to Table 2 for the JE-990 operational amplifier operating from a  $\pm 24\text{-V}$  supply, delivering an rms output voltage of 14 V into an open circuit, except for test G where a 150- $\Omega$  load is used.

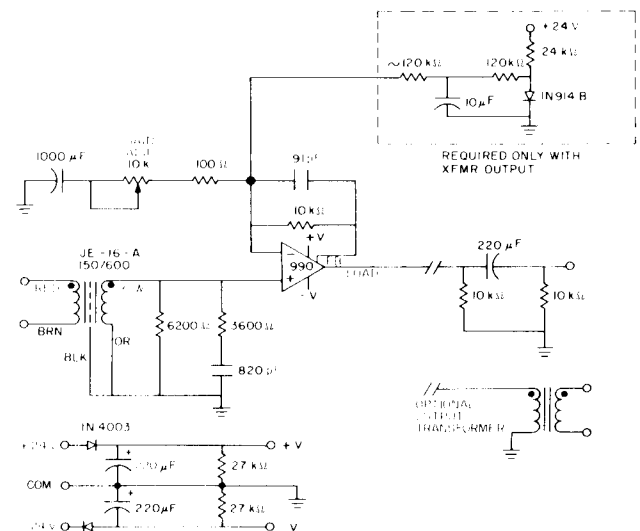


Fig. 13. Microphone preamplifier with offset compensation and adjustable gain.